



## Research papers

# Quantifying temporal variability and spatial heterogeneity in rainfall recharge thresholds in a montane karst environment

Andy Baker<sup>a,\*</sup>, Mirjam Scheller<sup>b</sup>, Fabio Oriani<sup>c</sup>, Gregoire Mariethoz<sup>c</sup>, Andreas Hartmann<sup>b,a</sup>, Zhangyong Wang<sup>d</sup>, Mark O. Cuthbert<sup>a,e</sup>

<sup>a</sup> Connected Waters Initiative, UNSW Sydney, NSW 2052, Australia

<sup>b</sup> Chair of Hydrological Modeling and Water Resources, Albert-Ludwigs-University of Freiburg, Friedrichstraße 39, D-79098 Freiburg, Germany

<sup>c</sup> Institute of Earth Surface Dynamics, Faculty of Geosciences and Environment, University of Lausanne, Geopolis, CH-1015 Lausanne, Switzerland

<sup>d</sup> Key Laboratory of Desert and Desertification, Northwest Institute of Eco-Environment and Resources, Chinese Academy of Sciences, Lanzhou, China

<sup>e</sup> School of Earth and Environmental Sciences, Cardiff University, Cardiff, CF10 3AT, UK



## ARTICLE INFO

This manuscript was handled by Corrado Corradini, Editor-in-Chief, with the assistance of Stephen Worthington, Associate Editor

**Keywords:**

Groundwater  
Rainfall recharge  
Karst hydrology  
Cave drip water  
Bucket models

## ABSTRACT

Quantifying rainfall recharge thresholds, including their spatial and temporal heterogeneity, is of fundamental importance to better understand recharge processes and improving estimation of recharge rates. Caves provide a unique observatory into the percolation of water from the surface to the water table at the timescale of individual rainfall recharge events. Here, we monitor nine infiltration sites over six years at a montane cave site in south eastern Australia. Six of the drip hydrology time series have up to ~100 hydrograph responses to rainfall over the monitoring period, three sites do not respond to rainfall events. We use two approaches to quantify rainfall recharge thresholds. At an annual timescale, for all nine drip sites, the total annual percolation water volume was determined for each year of data. Daily rainfall recharge thresholds were then determined by maximising the correlation of annual percolation water volume and total precipitation above a variable daily threshold value. The annual recharge amount methodology produced rainfall recharge thresholds for seven sites, where high and significant correlations (rank correlations > 0.75) occur for daily precipitation thresholds between 6 mm and 38 mm/day. No rainfall recharge thresholds could be obtained from one site which had a low and constant annual drip amount, and from one site which exhibited ‘underflow’ behaviour. At an event timescale, for the six sites which had a hydrograph response to rainfall, the 7-day antecedent rainfall amounts were determined. Minimum 7-day precipitation amounts prior to a hydrograph response for specific drip sites were in the range 13–28 mm and 75% of all recharge events had a 7-day antecedent precipitation between 20.7 and 38.1 mm. Combining all drip water monitoring sites and analysing the data by month identifies a seasonal variability in the minimum 7-day antecedent precipitation necessary to generate potential recharge, from 15 to 25 mm in winter to >50 mm in February and March. We apply a simple water budget model, driven by P and ET and optimised to the observed potential recharge events, to infer a ‘whole cave’ soil and epikarst storage capacity. This storage capacity is between ~50 mm (using potential evapotranspiration, 92% of events simulated successfully) to ~60 mm (using actual evapotranspiration, 79% of events simulated successfully). Modelling of individual drip sites identifies spatial heterogeneity in soil and epikarst storage capacities. Our approach using multiple methodologies allows the comparison between both daily and weekly rainfall recharge thresholds and modelled soil and epikarst storage for the first time.

## 1. Introduction

Groundwater recharge is the “downward flow of water reaching the water table, adding to groundwater storage” (Healy, 2010). Recharge is diffuse (precipitation-generated infiltration through the unsaturated

zone, occurring over large areas) or focused (from losing or ‘leaking’ rivers, wetlands and lakes, and the base of closed depressions in karst areas) (Scanlon et al., 2002). The rainfall recharge threshold is the amount of precipitation that is required to overcome a combination of evapotranspiration losses and sub-surface moisture deficits which

\* Corresponding author.

E-mail address: [a.baker@unsw.edu.au](mailto:a.baker@unsw.edu.au) (A. Baker).

<https://doi.org/10.1016/j.jhydrol.2021.125965>

Received 11 September 2020; Received in revised form 1 December 2020; Accepted 4 January 2021

Available online 12 January 2021

0022-1694/© 2021 The Authors. Published by Elsevier B.V. This is an open access article under the CC BY license (<http://creativecommons.org/licenses/by/4.0/>).

control the initiation of vertical drainage of water. Downward water movement to the groundwater is therefore only possible at precipitation amounts above the range of recharge thresholds that can occur at any one location, depending on spatial heterogeneity of soil and bedrock and antecedent climate conditions. Many techniques are available to quantify recharge thresholds, for example using water isotopes, water table fluctuations, chlorine mass balance (Crosbie et al., 2010; Jasechko, 2019). In general, these are limited to monthly or lower resolution, with uncertainty in both the source and timing of groundwater recharge.

Caves situated in the unsaturated zone can be used as observatories for the movement of water from the surface to the aquifer. Uniquely, at the temporal resolution of individual recharge events, they can provide evidence of the infiltration of water at the ground surface and its subsurface movement towards the aquifer as potential recharge, and can do so at spatially discrete locations within and between caves. High-temporal frequency, continuous discharge time series of drip water infiltrating into caves was recently demonstrated for the first time as an unsaturated zone physical method (Healy, 2010) that can identify rainfall recharge thresholds (Baker et al., 2020). In a subtropical karst region, over a five-year monitoring period, thirty-one recharge events, identified by increases in drip discharge, were compared to surface precipitation records and a simple water balance model to quantify rainfall recharge thresholds and soil and karst storage capacity. However, due to the heterogeneity of water movement through karstified limestone, not all cave percolation waters exhibit an increase in drip discharge after recharge-generating precipitation events. For example, waters percolating from well-mixed, large-volume karst water stores may have low variability in discharge rate over time. Other percolation waters may be generated from 'overflow', 'underflow' or 'bypass' flow behaviour, as karst water stores fill and overflow, are bypassed, or are drained. In these cases, it would be advantageous to have alternative

methodologies to determine recharge thresholds, and their spatiotemporal heterogeneity.

To investigate this further, in this study we analyse nine drip water time series from the montane South Glory Cave in the Snowy Mountains of New South Wales, Australia. The recharge sites have been monitored from 2013 to 2019, with near-continuous time series. Data gaps in the hydrology time series are infilled using a resampling method based on multiple point geostatistics (see Section 3), the first application to cave drip water time series. We consider two methods to determine rainfall recharge thresholds. For the first, following Barron et al. (2012), the total annual recharge amount is compared to total annual precipitation for a range of specific daily rainfall thresholds using correlation analysis. This approach is now applied for the first time due to the possibility of using the data infilling methodology. The second method follows that of Baker et al. (2020), where recharge events recorded in hydrology time series are compared to the antecedent 7-day cumulative rainfall amount to obtain a 7-day rainfall recharge threshold. The large number of recharge events identified over the 6-year monitoring period allows the quantification of monthly variability in rainfall recharge thresholds for drip water hydrology time series for the first time. This is second application of cave drip water hydrology time series to determine rainfall recharge thresholds, and the first for a montane climate. We apply a simple water budget model, driven by P and ET and optimised to the observed recharge events, to infer a 'whole cave' soil and epikarst storage capacity. Observed rainfall recharge threshold amounts using two methods are compared to modelled soil and karst water storage amounts, the first comparison between modelling and two rainfall recharge threshold methodologies. The spatial heterogeneity of both recharge thresholds and modelled soil and karst water storage is quantified.

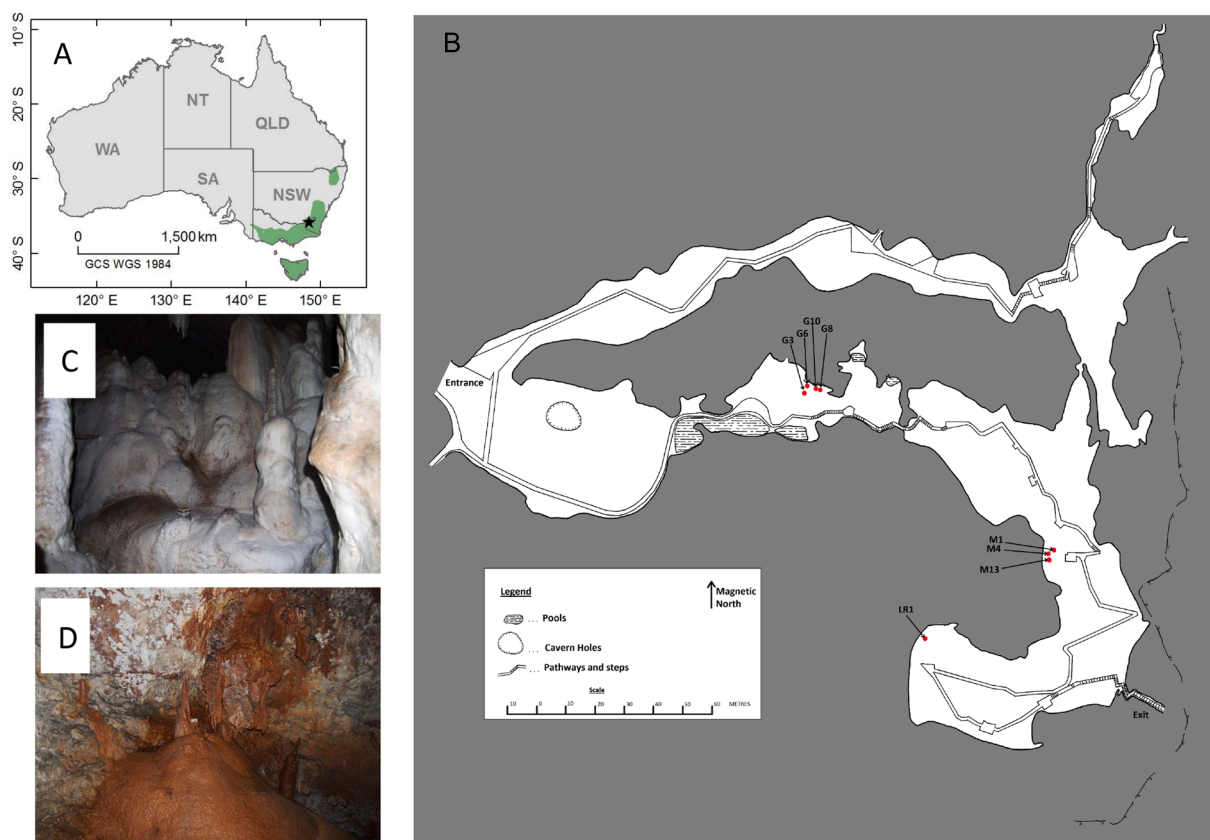


**Fig. 1.** (A) Location of Yarrangobilly Caves in New South Wales, Australia. Extent of Köppen climate zone Cfb is from Peel et al. (2007). (Coleborn et al 2016). (B) Glory Hole Cave survey, with location of loggers in South Glory Cave shown. Logger M14 is not shown as it is situated at the same location as M13. (C) Drip water percolation site G3 indicated by the location of the drip logger (D) Percolation site LR1 indicated by the location of the drip logger.

## 2. Site description

South Glory Cave is one of the two Glory Hole Caves of Yarrangobilly Caves, in the Snowy Mountains of New South Wales, Australia (Fig. 1), located at 35° 43' 29.3" S, 148° 29' 14.9" E and an elevation of 980 m (Australian Height Datum) and within the Kosciuszko National Park. The Snowy Mountains form part of the Great Dividing Range, a mountainous region along the eastern seaboard of Australia. The climate is classified as temperate montane with mild summers and no dry season (Köppen climate classification Cfb) (Peel et al., 2007). The region experiences bushfires, most notably the Canberra 2003 fire and in 2020. During the monitoring period, a low intensity hazard reduction burn was undertaken (in 2015). Hydrological monitoring of percolation water at South Glory Cave has the potential to inform other research at Yarrangobilly Caves, which has predominantly focussed on understanding the potential paleoclimate record contained in cave drip waters (Markowska et al., 2015; Campbell et al., 2017; Tadros et al., 2016, 2019) and speleothems (McGowan et al., 2018).

Glory Hole Cave is ~243 m in length and is ~100 m at its widest point. The cave extends to more than 40 m below the surface in the unsaturated zone of west-sloping ridge formed from limestone bedrock (Fig. 2A). The ridge is approximately 700 m wide, bounded to the south

by an E-W orientated valley and to the north by a NE-SW orientated valley. The local topographic high for the ridge is 1.4 km to the NE. Both bounding valleys have streams (Rules Creek, Mill Creek) that sink to the east of the cave. Dye tracing has shown a recharge pathway for both creeks through to cave streams in River Cave and Federation Cave (Spate et al., 1977), caves located close to the Yarrangobilly River (Fig. 2B). The estimated contributing catchment for South Glory Cave comprises the overlying limestone, and possibly also the higher topography to the NE by lateral flow. The cave is situated within limestone of Silurian age, highly fractured and marbleised with little primary porosity. Overlying the cave is a sub-alpine open snow gum woodland with *Eucalyptus pauciflora* subsp. *pauciflora* and black sallee (*E. stelullata*) (Coleborn et al., 2016). Soil cover at Yarrangobilly is discontinuous and varies with slope and karstification, and includes red clay sequences with A and B horizons of up to ~30 cm depth and thin loose soils with a single horizon (Baker et al., 2019). The extent of the epikarst is unknown. Long-term drip water monitoring in three sections of the cave (designated LR, G, M) was established in 2012 and is ongoing. In the early monitoring period, diurnal variability in drip water percolation rate was observed at some locations, most commonly in late summer, with decreased drip rates in late afternoon and evening, and attributed to tree water use (Coleborn et al., 2016). Drip water major ion, trace element and isotope geochemistry analyses at the same long-term monitoring locations identified well-mixed waters with negligible water stable isotope variability over time and no impact from the 2015 hazard reduction burn (Coleborn et al., 2018; 2019).

Nine monitoring sites were selected for analysis (G3, G6, G8, G10, LR1, M1, M4, M13, M14). These sites had the most continuous hydrological time series and are a subset of the twelve sites previously analysed for diurnal variability (Coleborn et al., 2016). All monitoring sites were supersaturated with respect to calcium carbonate and had associated speleothem formations. The type of speleothem can inform on the hydrological flow regime, with stalagmites likely to have lower or less variable water fluxes amounts compared to flowstones. Percolating waters at M1 and M4 were precipitating stalagmites, all other monitored percolation waters were precipitating flowstones. Monitoring sites M13 and M14 are less than 2 m apart. The flowstone associated with site LR1 is notably brown in colour (Fig. 1d), in contrast to the white colour of the speleothems associated with the other monitoring sites (for example, Fig. 1c). The brown coloration likely indicates the presence of chromophoric organic substances and associated organic-bound metals, and a greater soil connectivity compared to other monitoring sites.

## 3. Methodology

Daily precipitation data was obtained from the Australian Bureau of Meteorology station located at Yarrangobilly Caves (ID 072141, data available at bom.gov.au/climate/data). Percolating drip water was monitored using Stalagmate © loggers (Collister and Matthey, 2008). The number of drips in 15 min was recorded, with logger memory allowing recording ~11 months of data. Data was downloaded from the loggers every 6–11 months, with data gaps occurring due to logger failure, logger dislocation, or inability to access the caves.

Missing data are present for 6.9% of the drip time series, occurring in continuous gaps up to months long, corresponding to temporary logger failures. The gaps are infilled using a Multiple-Point Statistics (MPS) technique. MPS, already used to simulate and infill hydrological time series (Oriani et al., 2014, 2016; Dembele et al., 2019), is a stochastic simulation approach that generates random data patterns by mimicking the ones present in a training dataset, which in this case is constituted by the available data from the same time series. In particular, a recent MPS algorithm is used here, called QuickSampling (QS) (Gravey and Mar-ethoz, 2020), which generates the missing data with a simple resampling scheme: the data in the neighbourhood of a missing (target) time step are retrieved and a similar data pattern is searched in the same time series. A random pattern among the most similar  $k$  ones found is then

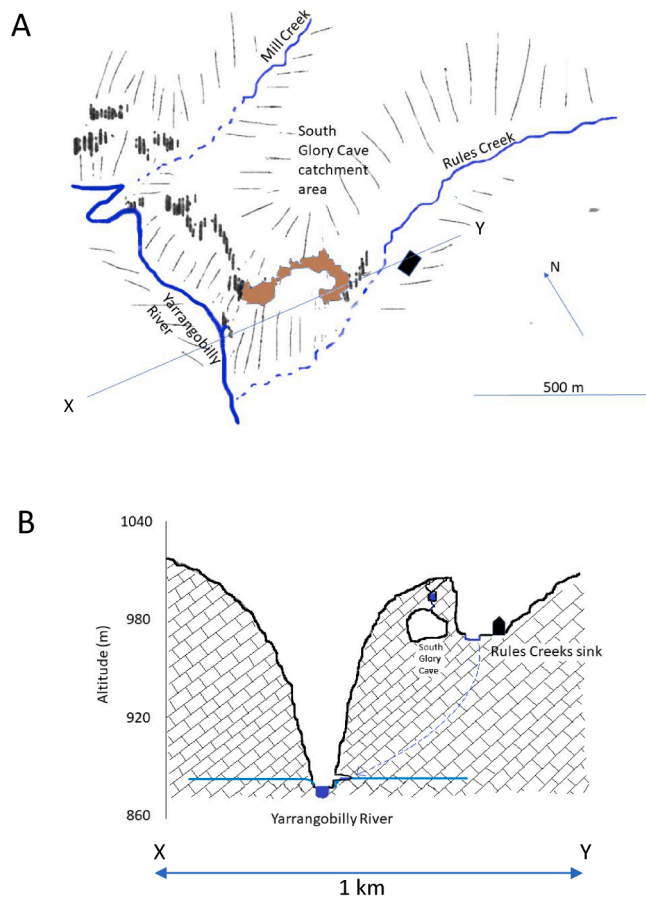


Fig. 2. Conceptual figure of the unsaturated zone hydrology at South Glory Cave. (A) Sketch map showing the location of South Glory Cave (in brown) relative to the local streams and valleys. The transect XY is presented in (B), and passes through the Yarrangobilly River, River Cave, the eastern part of South Glory Cave, Rules Creek sink and the Yarrangobilly Caves House (solid black rectangle). (B) Section (vertical axis scale exaggerated) showing the E-W dipping limestone, the Yarrangobilly River, the inferred position of the groundwater level and unsaturated zone water flow from the surface creeks to the Yarrangobilly River, emerging in the River Cave and Federation Cave systems. A perched water source is shown above South Glory Cave.

chosen and the datum at its centre is assigned to the target time step. The procedure is repeated for all missing data in a random order, until the time series is complete. In this way, the generated data patterns preserve a realistic structure in continuity to their neighbour data. In addition to the cited previous works that demonstrate the efficacy of the approach in this kind of application, preliminary cross-validation experiments have been performed on the present dataset. For more details about the setup chosen and its validation see Supplemental Information (Methods, including [Figures S1 and S2](#)).

Total annual percolation water amount is determined for all nine drip water monitoring sites for the period 2013–2019. We recognise that caves form part of a preferential flow system through the limestone, and it is difficult to relate the percolation volume observed in the cave to that which might occur in the wider karst system. Visual inspection of the drip rate time series showed that the hydrological year starts in April, with an increase in drip rates occurring in all years after a late summer drip recharge minimum. Therefore, total annual percolation water amount was determined from the 1st of April to the 31<sup>st</sup> of March. Annual amount in litres is compared to total annual precipitation amount in mm for different daily total precipitation thresholds (>0 mm to >50 mm/day). A Spearman's correlation matrix is used to determine the daily precipitation threshold with the strongest correlation to total annual percolation water amount.

Visual inspection of the drip hydrology time series showed that six of the nine monitoring sites exhibited a hydrograph response, as opposed to the other three sites which had relatively smoothed and temporally autocorrelated drip rate time series. For these sites, the timing of hydrograph response was compared to the 7-day antecedent precipitation, following the methodology of [Baker et al. \(2020\)](#). To determine rainfall recharge thresholds, the 7-day antecedent precipitation was determined for the days prior to, and including, the day of recharge. This approach accounts for the effect of a prolonged rainfall period on recharge ([Barron et al., 2012](#)) and allows for potential retardation of water flow through epikarst water stores. The antecedent precipitation over timescale great than 7-day was not considered as the majority of precipitation events have a duration of 1–4 days, and frequency of precipitation events associated with frontal systems associated with the mid-latitude westerly zonal circulation is ~7–14 days in winter. Potential recharge events were defined as occurring whenever (1) drip rates first increase from a baseline rate and (2) the drip water response has the properties typical of a karst hydrological response (e.g. rapid increase in drip rates, with varied patterns of drip rate decrease). We excluded MPS infilled sections of the timeseries for this analysis. Since caves form part of a preferential flow network in karst systems, we expect that the rainfall recharge thresholds determined by this method will be lower than those experienced outside of zones of preferential flow. Descriptive statistics for the rainfall recharge thresholds for each drip water recharge sites, and for all sites for each month of the year, were derived.

Daily precipitation and evapotranspiration data were used as input of a simple soil and karst water budget model, which was used to quantify the soil and karst water storage capacity. The model is described in detail in [Baker et al \(2020\)](#) and is available at [github.com/KarstHub/Simple-Water-Budget-Model](https://github.com/KarstHub/Simple-Water-Budget-Model), where the model structure is also presented. The model is forced on a daily time step with daily precipitation [P, mm/day] and daily evapotranspiration [mm/day]. For comparison, we use both actual (AET) or potential (PET) evapotranspiration [mm/day] as model inputs, due to uncertainties associated with AET data. Actual and potential evapotranspiration are obtained from the Australian Water Resources Assessment Landscape model (AWRA-L) version 6.0 ([Viney et al., 2015](#); [Frost et al., 2018](#)). AWRA-L is a daily, distributed water balance model at 0.05° (~5 × 5 km) resolution, which simulates water flow through vegetation, upper and lower soil moisture stores and a groundwater store, with model outputs which include actual and potential evapotranspiration, runoff and deep drainage ([Frost and Wright, 2018](#)). Actual Evapotranspiration is estimated from: (1)

water evaporated directly from the canopy interception, the upper soil water store and the groundwater store; (2) water loss by transpiration from the lower soil water store, the deep soil water store and the groundwater store.

In our simple water budget model, two 'free' parameters have to be determined, the overflow capacity [mm] and a drainage parameter [mm/day]. The overflow represents the threshold that initiates fast and concentrated recharge [mm/day] to the cave, after field capacity of the soil and epikarst has been reached. The two free parameters are optimised on the observation of recharge within a 7-day window of a precipitation event, to minimise the difference between observed recharge events and modelled concentrated recharge. A 7-day window was allowed as the timing of recharge at the different monitoring sites was observed to vary by several days, likely due to the time taken for karst water stores to fill and overflow. The window length of seven days was found most suitable by a trial-and-error procedure using windows lengths up to 10 days. Modelled estimates of the overflow capacity and drainage parameters are returned for this optimised solution. The model was optimised to simulate the observed recharge events for: (a) the 'whole cave', for all recharge events identified at the cave, obtain an overall soil and epikarst storage amount and also (b) for each individual monitoring site, to quantify heterogeneity in modelled soil and epikarst storage capacity.

#### 4. Results

In the following section, we will examine the considered drip site time series together with the associated weather record, we present the estimation of rainfall recharge thresholds and the water budget model of the site.

[Fig. 3](#) presents a comparison of time series for precipitation ([Fig. 3a](#)), modelled AET ([Fig. 3b](#)), cumulative P-AET ([Fig. 3c](#)). Precipitation events that are associated with drip recharge events are highlighted ([Fig. 3a](#)). The site shows that cumulative P-AET increases over the six years of monitoring ([Fig. 3c](#)), with an average increase of ~330 mm/yr (01/04/2013 – 31/03/2019). As we use both AET and PET as input terms to our karst water budget model, we also used modelled PET to calculate the cumulative P-PET. P-PET had a negative trend of ~180 mm/yr over the same time period.

The drip hydrology time series are presented in [Fig. 3d](#) (site LR1) and [Fig. 3e](#) (all other drips), and time series for all individual drip sites, including infilled sections, in [Figure S1](#). Drip site LR1 is presented separately, as visual inspection of the time series identified many more increases in drip rates at drip site LR1 compared to all the other monitored percolation sites. Several of the drip monitoring sites can be characterised as being flashy, with rapid increases in drip rate from a baseline (LR1, M4, M13, M14). Drip monitoring site G10 has a smooth annual variability in drip rate, with a rapid increase in drip rate at the start of each hydrological year, which occurs in late autumn (April/May). Sites M1, G3 and G6 have a smooth seasonal variability in drip rate, with no rapid increases in drip rate at the start of the year. Site M1 has low drip rates and a relatively invariant drip rate compared to the other sites. Sites G3 and G6 have flashy drip rate increases, predominantly during periods of increased drip rate, superimposed on the seasonal signal. Drip water monitoring site G8 has a contrasting time series to others, with relatively consistent drip rates which are more variable during higher drip rate periods.

The total annual percolation water amount for each of the drip sites is presented in [Table 1a](#), with drips summed for the hydrological year starting April, and converted to a volume assuming a constant drip volume of 0.15 ml/drip.

##### 4.1. Daily rainfall recharge thresholds determined using the annual percolation water amount –threshold precipitation correlation method.

Seven of the nine drip sites have statistically significant and positive

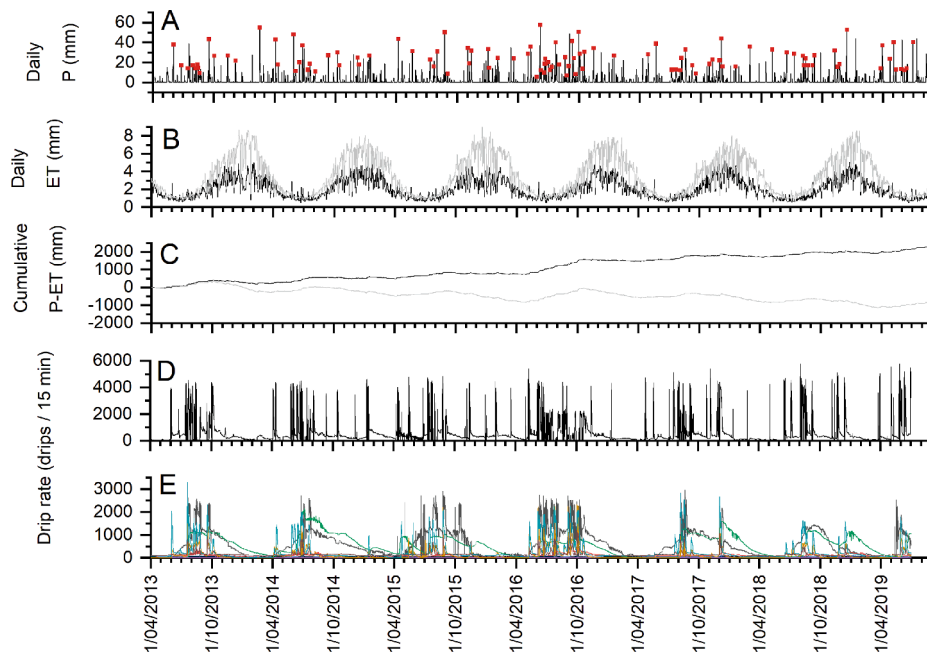


**Fig. 3.** (A) Daily precipitation (mm) with precipitation events associated with drip water recharge shown (red dots) (B) Daily AET (black line) and PET (grey line) (from Australian Landscape Water Balance model (C) Cumulative P-ET (AET – black; PET – grey). (D) Drip hydrology time series for flowstone LR1 (E) Drip hydrology time series for all other drips. (For interpretation of the references to colour in this figure legend, the reader is referred to the web version of this article.)

**Table 1**

(A) Total annual recharge for each drip site (B) Total annual precipitation (mm/yr) above a given daily rainfall amount.

(A) Total annual recharge (Litres)													
SUM LITRES													
	G3	G6	G8	G10	LR1	M1	M4	M13	M14				
1/4/13–31/3/14	2814.0	462.7	301.1	2410.9	2597.9	16.2	677.1	1281.7	811.2				
1/4/14–31/3/15	3103.3	367.6	286.1	4101.5	3008.5	21.6	570.0	1238.2	788.6				
1/4/15–31/3/16	3457.1	266.9	300.7	2251.7	3057.1	22.3	536.2	1075.3	761.7				
1/4/16–31/3/17	4203.1	721.6	323.4	2047.1	3090.4	17.1	1369.2	2079.9	989.0				
1/4/17–31/3/18	3110.4	581.9	212.2	3172.0	2677.5	20.2	338.5	1279.2	731.6				
1/4/18–31/3/19	2241.4	489.5	225.1	2679.8	2915.0	13.3	509.7	1149.8	548.0				
(B) Total annual precipitation above given threshold daily amount (mm/yr)													
	TOTAL	>4 mm	>8 mm	>12 mm	>16 mm	>20 mm	>24 mm	>28 mm	>32 mm	>36 mm	>40 mm	>44 mm	>48 mm
1/4/13–31/3/14	1017.8	931.6	797.5	653.1	509.9	329.6	307.6	175.4	175.4	175.4	98.6	55.0	55.0
1/4/14–31/3/15	1060.3	962.8	810.1	701.7	622.3	479.6	325.8	220.4	162.2	128.2	91.2	48.3	48.3
1/4/15–31/3/16	1025.7	919.9	776.1	638.6	556.5	449.5	315.6	291	196.8	93.9	93.9	50.2	50.2
1/4/16–31/3/17	1472.5	1367.1	1162	990.7	863.3	698.8	563.3	486.8	308.3	238.3	198.3	156.9	156.9
1/4/17–31/3/18	1014.6	915.9	756.2	656.4	506.2	367.6	322.2	223.0	194.8	126.0	87.0	0	0
1/4/18–31/3/19	1027.0	921.0	786.5	605.2	484.3	414.1	392.7	288.2	199.2	134.0	97.0	97.0	52.8

correlations with annual precipitation above a specific daily precipitation threshold amount (Fig. 4, Table 1b). Only one drip site (LR1) has statistically significant correlation between total annual precipitation and percolation water amount (Spearman’s rank correlation,  $r_s = 0.77$ , significant at 95% confidence level). This site has a higher correlation between total annual percolation water amount and precipitation for a daily precipitation recharge threshold of 20 mm ( $r_s = 0.94$ , significant at 99% confidence level) (Fig. 4). For these seven sites, high and significant

correlations (all  $r_s > 0.75$ , significant at a 95% confidence level) occur for daily precipitation thresholds which range from a minimum of between 6 mm (M4, M14) and 38 mm (G6, M13) and up to a maximum of 46–50 mm (G8, M4) (Fig. 4, Table 1b). The results from these seven sites suggest that 6–38 mm is the range of minimum recharge thresholds for daily precipitation at South Glory Cave. Supplementary Figure S3 shows the relationship between annual percolation water amount and annual precipitation above the threshold value for the best correlation

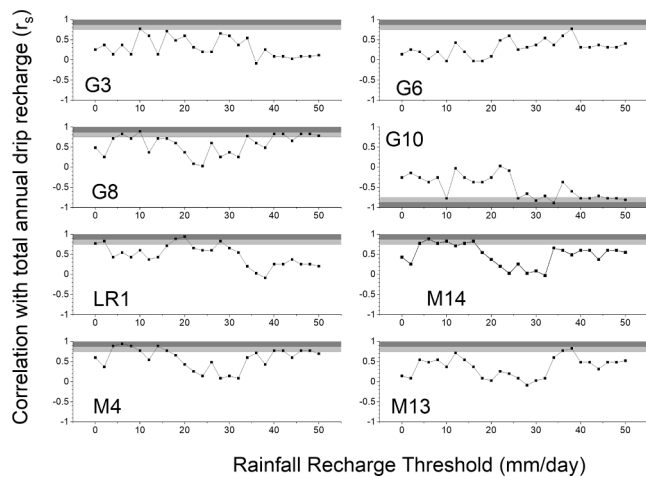


**Fig. 4.** Correlation between annual drip recharge and annual precipitation for various daily rainfall thresholds. Light and dark grey show the 95% ( $r_s > 0.75$ ) and 99% ( $r_s > 0.87$ ) confidence levels (positive correlation all drips except G10, where negative correlation confidence levels are shown).

threshold value for each drip water monitoring site.

One site, M1, has no significant correlations between annual percolation water amount and precipitation at any recharge amount. Site M1 has the lowest annual percolation water amount (~10 L/year), one order of magnitude lower than the next highest annual percolation water amount, with very little inter-annual variability (range 13.3 to 22.3 L). Site G10 has a significant negative correlation with precipitation for daily precipitation thresholds over 28 mm, with the strongest correlation with a daily precipitation threshold of 34 mm ( $r_s = -0.89$ ). This site is distinguished by its relatively smooth time series with no flashy drip rate increases and we interpret its recharge response to precipitation as underflow behaviour from a karst store.

**4.2. 7-day rainfall recharge thresholds using hydrograph response methodology.**

Over the six-year period, individual drip sites had between 21 (site G10) and 102 (site LR1) hydrograph responses and inferred potential recharge event (averaging between 3.5 and 17 recharge events a year) (Table 2). The greatest number of hydrograph responses are found at the four sites characterised by flashy increases in drip recharge (LR1, M4, M13 and M14), with most events for the LR1 drip water precipitating the brown-coloured flowstone, the colour indicative of a significant soil-water connectivity. Minimum 7-day precipitation amounts prior to a hydrograph response for specific drip recharge sites were in the range

**Table 2**

Number of recharge events per month identified in the six drip hydrology time series (LR1, M4, M13, M14, G3, G10). No recharge events occurred from 1/4/13 to 1/7/13. Percentage of all sites recharging in a specific month. Median and minimum 7-day antecedent precipitation for each month.

	Number of recharge events per month (1/7/2013 – 30/6/2019)				Median 7-day Precipitation (mm)			Minimum 7-day precipitation (mm)		
	All sites	Site LR1	All sites except LR1	Percentage of sites recharged (excluding LR1)	All sites	Site LR1	All sites except LR1	All sites	Site LR1	All sites except LR1
J	10	6	4	80	64.4	55.85	107.35	29.8	42.6	29.8
F	3	2	1	20	65.7	70.15	65.7	53.7	53.7	65.7
M	3	3	0	n/a	56.9	56.9	>81	36	36	>81
A	13	5	8	53	50.8	50.8	49.75	23.6	23.6	39.6
M	28	11	17	68	47.9	37.2	50.9	14.9	14.9	20.9
J	53	14	39	75	60.2	60.4	60.2	16.6	16.6	22.1
J	56	12	44	80	31.4	28.75	34.4	20.1	20.1	20.1
A	69	16	53	71	39.1	37.8	39.1	17.4	17.4	19.4
S	43	10	33	73	63.6	28.25	63.6	13.3	13.3	24.4
O	19	7	12	60	44.3	32	45.35	16.8	16.8	35
N	19	10	9	45	47	43.35	49.8	23.6	23.6	40.8
D	16	6	10	67	92.7	65.15	92.7	41	41	41.2

13.3 (LR1) to 28.2 mm (G10) and 75% of all recharge events had a 7-day antecedent precipitation between 20.7 (LR1) and 38.1 mm (G3) (Fig. 5).

Combining all recharge sites and analysis by month of hydrograph response shows a seasonal variability in the minimum 7-day antecedent precipitation necessary to generate potential recharge events, from 15 to 25 mm in winter to > 50 mm in February (Fig. 6). No potential recharge to stalagmite drips was observed over the monitoring period in March, with an inferred minimum 7-day precipitation threshold of 81 mm based on the maximum 7-day precipitation total over our monitoring period.

Overall, the 7-day rainfall recharge minimum thresholds of between 13.3 and 28.2 mm, varying between sites, correspond well to the amount and variability in the daily rainfall recharge thresholds of between 6 and 38 mm. However, monthly variability in 7-day rainfall recharge thresholds is greater than that observed between-sites for the annual average 7-day rainfall recharge threshold.

**4.3. Water budget modelling to quantify soil and karst storage.**

Water balance modelling was applied using both P and AET and P and PET as input data, optimising the model to generate overflow from the soil and epikarst store to agree with observed occurrence of cave drip water recharge events. To understand the general cave hydrological characteristics, we undertook modelling of a combined observed cave drip water dataset, for any occasion where recharge was observed at any of the monitoring sites excluding LR1. We also undertook modelling for each individual drip site. Fig. 7 shows the timeseries of observed recharge events for the combined drip water dataset, model input

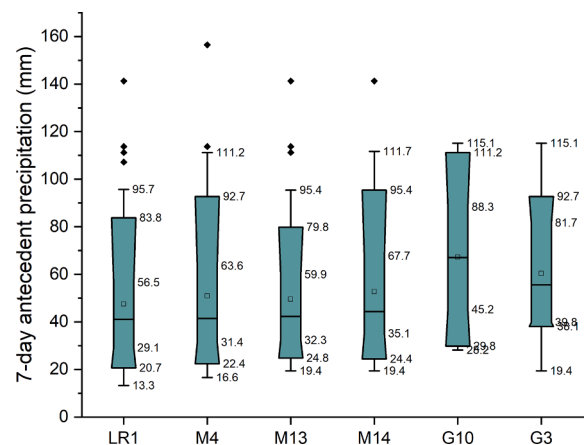


**Fig. 5.** 7-day antecedent precipitation for all events generating recharge for six drip sites. Values for the maximum, minimum, median, and inter-quartile range are shown. Outliers are shown as diamonds, the average as an open square.

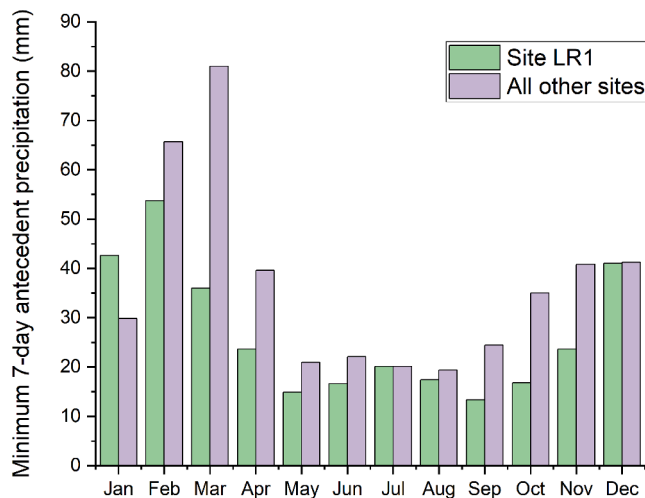


Fig. 6. 7-day minimum antecedent precipitation necessary for recharge for each month. Note that no stalagmites recharged in March over the study period, and the value shown is based on the highest observed 7-day precipitation over the time.

parameters, and simulated recharge events showing fit and misfits to the model. Model fit to the combined recharge events shows that similar results are obtained using either AET or PET as an input parameter. This is because at the daily timescale there is little difference in PET and AET in winter, when the majority of recharge events occur, and for recharge-inducing events in summer, daily AET can also approach PET due to the extra moisture available for transpiration. The overflow capacity of the soil and epikarst varies from  $\sim 50$  mm (using PET, 92% of events simulated successfully) to  $\sim 60$  mm (using AET, 79% of events simulated successfully). These values are slightly greater in amount than the hydrograph-derived 1-day average and 7-day minimum rainfall recharge thresholds indicating that the model is more representative of a larger diffuse recharge component than is captured by the cave monitoring.

A summary of the fit and misfits between the combined drip water observed recharge and simulated recharge is provided in Table S1. Investigation of this data provides further insights into the recharge processes occurring at the site. The simulated recharge events occurred mostly after the observed recharge (for 9 of 14 events), and outside the 7-day window applied in the model. This suggests that percolation waters can arrive rapidly at the cave, via a pathway that by-passes the soil and karst store. For example, this could be generated by quick runoff from intense rainfall events which can activate by-pass recharge pathways. For 2 out of the 14 events, recharge was simulated but observed only at the site LR1. The final 3 occasions where recharge was simulated and not observed occur during April–June 2015, around the time of the first recharge events of the hydrological year, and suggest the model misfits are due to uncertainties in model input terms or model structure as it reaches overflow capacity for the first time. Six observed recharge events were not simulated, and for most of these events, recharge was only observed at one site (M4). This suggests a different recharge pathway at this site, potentially from a by-pass flow contribution or a smaller soil and epikarst water storage or drainage term than the other sites.

Individual sites were also modelled: modelled overflow capacity and drainage terms are presented for the simulations using AET in Fig. 8, and the time series of observed and simulated recharge events are shown in Supplementary Figure S4. We see a poorer model fit for individual sites compared to the combined dataset, but, despite this, our analyses elucidate a spatial heterogeneity in overflow capacity. This is most notable for drip site LR1, which has lower modelled overflow capacity, in agreement with the lower rainfall recharge threshold for this site.

Modelling suggests the absence of a significant karst water store and a lower overflow capacity, and this would agree with the interpretation of the associated brown-coloured flowstone indicating the dominance of the soil water store. Drip site G10 has the lowest model fit. An optimum solution cannot clearly be selected. Model results did not change significantly with different drainage or overflow capacity values. Although, compared with the other sites rather high drainage values are emphasised. Site M4 has a similar model optimum solution to other sites, suggesting the failure to simulate some recharge event at this site is due to the model over-simplifying the recharge process, for example by-pass flow that routes some water past the soil and epikarst store to the cave.

## 5. Discussion

We apply two different methodologies on the same dataset to quantify daily rainfall recharge thresholds. In both methodologies, we cannot determine the surface catchment area for the potential recharge that we observe as cave percolation waters, which would require the use of tracer tests. In addition, as cave systems form part of preferential flow pathways through karst, we note that the recharge thresholds we determine best relate to the preferential flow pathways.

The annual percolation water volume amount methodology has the advantage that it can be applied to all drip water hydrology time series, including those with little or no hydrograph response to recharge events, and that it can generate a daily rainfall recharge threshold value for multiple percolation sites. We hypothesise that percolation waters with relatively smoothed hydrographs would become more common in deeper caves where percolation waters would have a greater potential to have previously experienced storage and mixing, and that this approach would be of utility. However, at this stage of development, the technique is limited to annual-average daily recharge threshold value, when it is expected that this threshold will vary sub-annually with antecedent climate conditions. In addition, the technique requires long-term monitoring datasets; here a minimum of six years is shown to be sufficient, but longer time series would be advantageous.

The MPS approach used to infill the missing data in the water drip time series is demonstrated to be a convenient technique to obtain a continuous signal from incomplete but representative records. However, the application on very large data gaps, typically larger than the correlation length of the time-series, (see the sample autocorrelation function Supplementary Figure S5) or very patchy datasets should be carefully considered, since the technique can only use the data patterns present in the same time series. In those cases, it may not reconstruct the data structure reliably or generate long-recurrence-time events. For the latter purpose, models focussed on extreme events may be a more reliable approach.

The annual recharge amount methodology only produced rainfall recharge thresholds in 7 out of 9 cases, and could not be applied to one site with low annual drip amount and low drip rate variability (site M1), and one drip hydrograph with high autocorrelation (G10, Figure S5) with an inferred ‘underflow’ behaviour. The range of annual-average daily rainfall recharge thresholds from 6 to 38 mm determined from this methodology agrees with the 7-day minimum rainfall recharge thresholds determined using the hydrograph response methodology (13.3 to 28.2 mm annual average; ranging from 15 to 25 mm in winter to  $> 50$  mm in late summer).

The comparison of hydrograph responses to antecedent 7-day precipitation requires sufficient recharge events to produce a large enough dataset of antecedent conditions to reliably determine a minimum precipitation amount. At our montane climate site, this was achieved over a six-year monitoring period, however long monitoring times might be necessary at more water-limited sites with less frequent recharge events. With sufficient hydrograph responses, monthly or higher resolution variations in recharge thresholds can be elucidated, as well as differences in recharge thresholds between drips, and the quantification of the

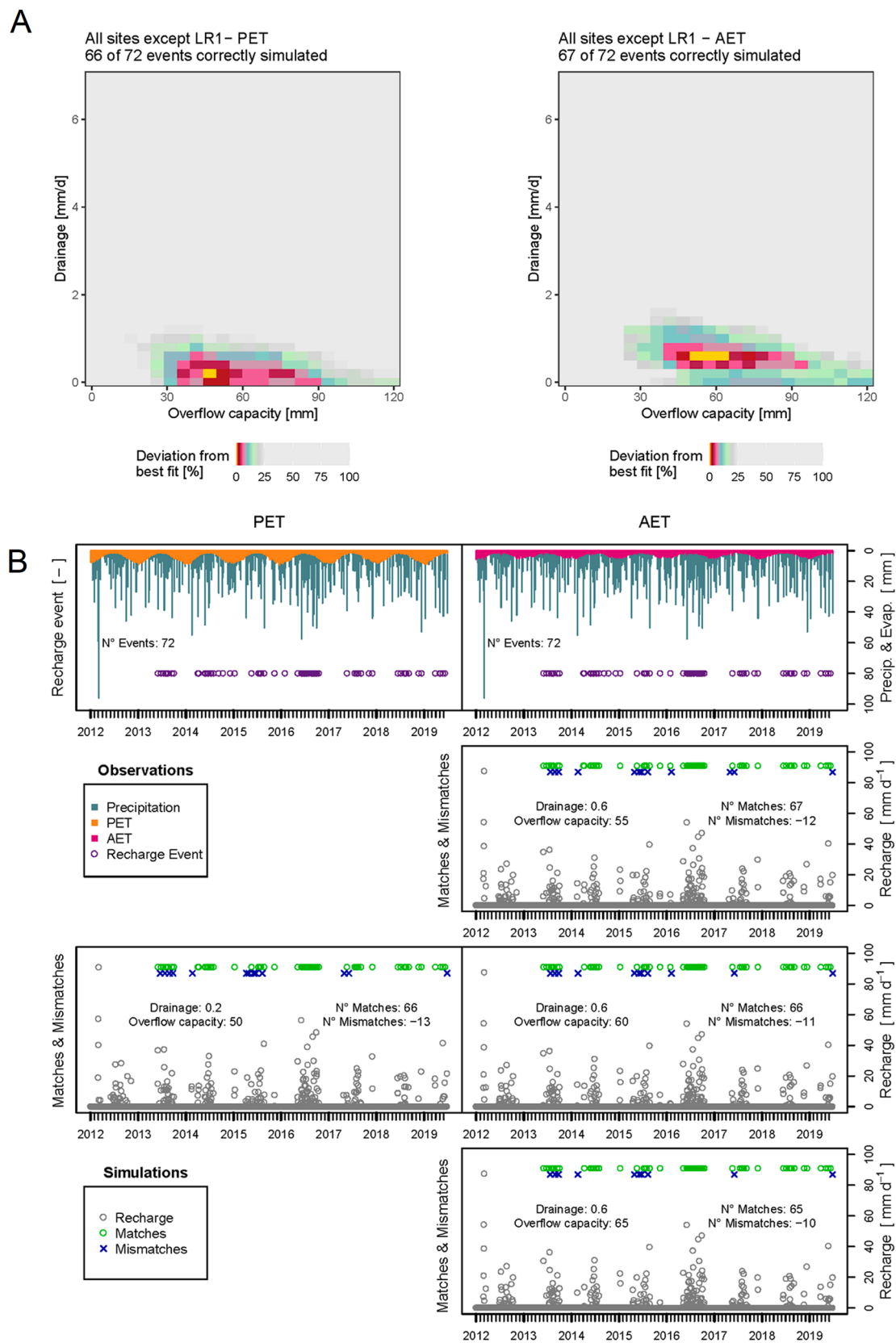


**Fig. 7.** (A). Soil and karst water balance model output for all combined drip recharge data. Left plot presents model solution using PET as an input parameter. Right plot using AET as an input parameter. Best fit is the yellow region. (B) Timeseries showing input data and optimal model solutions. The upper row shows the observational data. The lower rows present the optimal model solutions. The left column presents observation data and model solution using PET as an input parameter. Right column using AET as an input parameter using three different combinations of a drainage parameter of 0.6 mm/d and the three optimum values of the overflow capacity (55–65 mm). (For interpretation of the references to colour in this figure legend, the reader is referred to the web version of this article.)

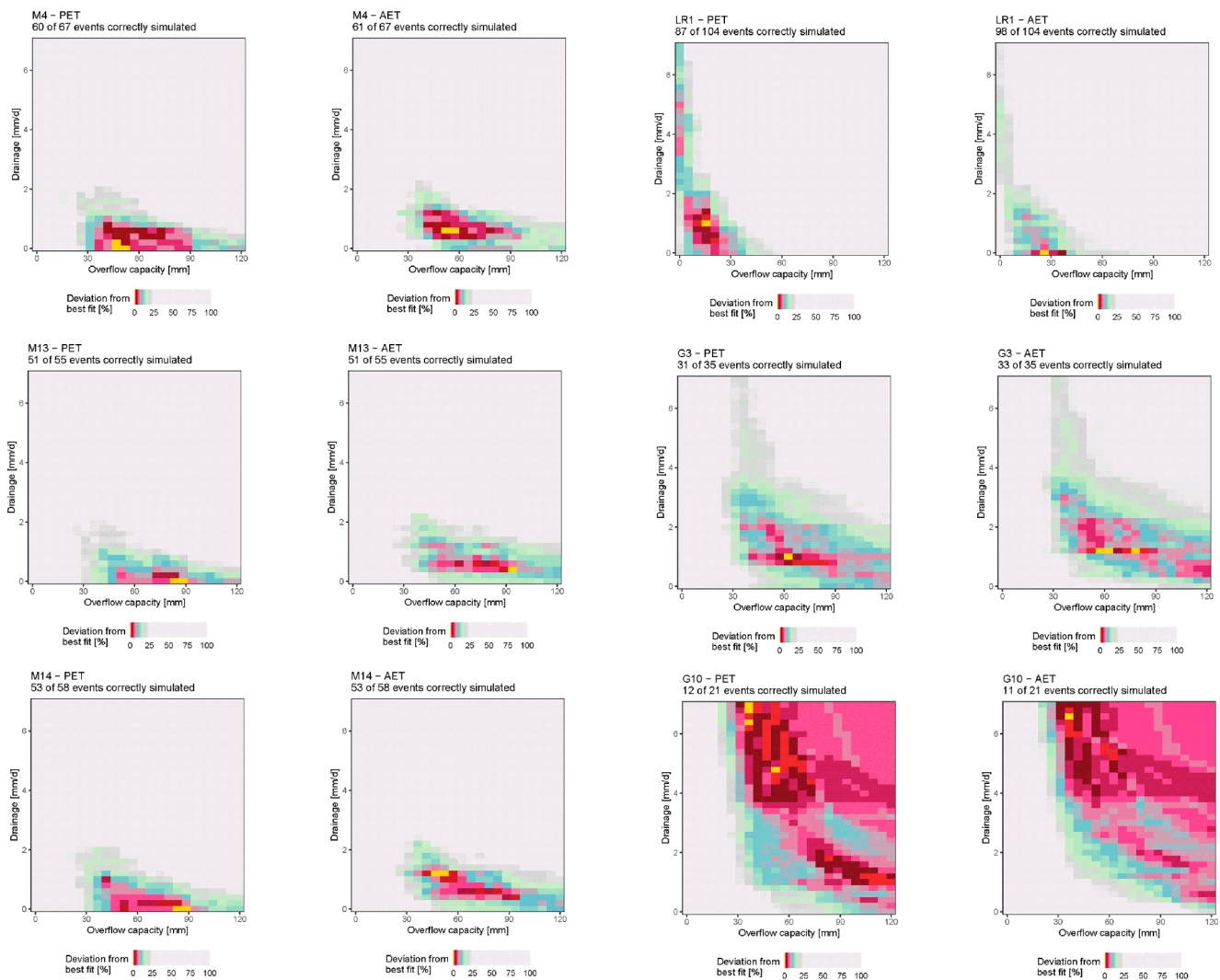


**Fig. 8.** Soil and karst water balance model output for individual drip recharge data, using both PET and AET as an input parameters. Best fit is the yellow region. (For interpretation of the references to colour in this figure legend, the reader is referred to the web version of this article.)

percentage of sites where potential recharge is observed for each month. The methodology can only work at drip sites where there is a hydrograph response, here just six of the nine monitoring sites, and we infer that this methodology is best suited to shallow caves where mixing and storage of water in the unsaturated zone is relatively limited. At South Glory Cave, the methodology was applied with a temporal resolution of 7-day antecedent precipitation, as this best accounted for the different lag times of individual drip site hydrograph responses to precipitation, and timing of precipitation within the 24-hour reporting period. Here, the minimum 7-day precipitation is  $> 50$  mm in late summer, due to high daily evapotranspiration rates which lead to greater rainfall amounts needed to reach soil field capacity and generate infiltration to the karst system. In winter, the minimum 7-day precipitation is  $> 10$ – $20$  mm, and in agreement with daily thresholds determined from annual recharge amount methodology (6 to 38 mm). In these cooler months with low daily evapotranspiration, we infer the soil moisture content is higher, and less rainfall is needed for the soil to reach field capacity and for infiltration to the karst to occur.

After imposing the rainfall-recharge thresholds on the rainfall time series of the study area, the corresponding infiltrated water amount has been estimated. We can compare our rainfall recharge thresholds. These can be used as a secondary evaluation of our physical model of the soil and karst overflow capacity. Using a simple water budget equation that requires just precipitation and evapotranspiration as inputs, optimised

on the basis of simulating the recharge timings as closely as possible, the soil and epikarst overflow capacity and drainage terms are quantifiable. The modelled soil and epikarst overflow capacity of  $\sim 50$ – $60$  mm, combined with a daily drainage of between 0 and 6.4 mm, is physically plausible at the event scale when compared to the observed 1-day average (6 – 38 mm) and 7-day minimum (15 – 25 mm in winter;  $> 50$  mm in summer) rainfall recharge thresholds. It also agrees with the observed little or no recharge in late summer when ET is highest and the soil moisture deficit greatest. Analysis of the misfits between model and observations suggest that a rapid, by-pass flow can occasionally generate potential recharge in the cave. This is a similar finding to our application of the same model to potential recharge observed in the Macleay karst, New South Wales (Baker et al 2020).

Combined with the results from previous studies of karst drip water hydrology and its relationship to recharge, our results help improve our understanding of karst water movement from the surface to the groundwater at different scales. At a local scale, the recharge thresholds determined here agree well to those estimated from comparison of soil moisture saturation and drip hydrology time series at the adjacent Harrie Wood Cave (13.0 – 31.4 mm /day; Markowska et al., 2015). At South Glory Cave, our observation that recharge is unlikely in late summer, due to larger moisture storage deficits driven by increased evapotranspiration, matches the timing of our observations of tree water use from karst stores and fractures. These were also only observed in late

summer, evidenced through diurnal drip rate variations, and indicative of trees accessing unsaturated zone water stores during periods of water stress (Coleborn et al. 2016).

In a national context, two contrasting karst regions have now been investigated using the same methodology. The minimum 7-day antecedent precipitation thresholds at the montane karst of South Glory Cave (13.3 to 28.2 mm) are lower than at those observed in caves in the Macleay Valley, mid-north coastal New South Wales (Lower Macleay, 33.3 mm; Upper Macleay, 30.1 mm; Baker et al., 2020). The Macleay Valley is a warmer sub-tropical region which experiences its greatest rainfall amount in late summer, with water percolation into the caves often observed in March due to rainfall associated with the southernmost extension of the summer monsoon trough. The Macleay cave monitoring sites also contrast to South Glory Cave in that they typified by thin to absent soil cover and subtropical rainforest vegetation. Despite different climatology, soil cover and vegetation type, modelled soil and karst water storage amount are comparatively similar at both sites (50–60 mm at South Glory Cave, 65 mm at Lower Macleay, 80 mm at Upper Macleay). This highlights the importance of the karst water store component of the soil/karst water stores. Our South Glory Cave results fall at the lower end of the range of storage capacities reported globally from other applications of simple bucket type models: 82–98 mm in Spain (Hartmann et al., 2013); 87 mm in NSW, Australia (Cuthbert et al., 2014); 70–190 mm in Jordan (Schmidt et al., 2014) and 70 mm in Texas, USA (Heilman et al., 2014). Comparison between the number and timing of hydrograph responses in our cave percolation waters, indicative of potential recharge, with modelled deep drainage from the Australian Landscape Water Balance (ALWB) Australian Water Resources Assessment Landscape Model (AWRA-L) model, is also possible. This model is a small catchment scale, gridded, distributed water-balance model with three soil water layers (upper, lower, and deep), with deep drainage the flux from the bottom of the deep soil layer (6 m) into the groundwater. This shows no relationship between observed recharge events and ALWB modelled deep drainage, which indicates a smooth sinusoidal variability in deep drainage with a summer minimum and winter maximum (data not shown). This is similar to observations at the Macleay and further confirms the lack of utility of modelled deep drainage to karst systems that permit rapid water movement through preferential flow routes. The extent to which represents deep drainage in karst systems away from preferential flow zones requires further investigation, for example through water level analysis of boreholes or springs, e.g. using observed spring hydrographs provided through the WoKaS database (WoKaS, Olaninoye et al., 2020).

In a global context, we can compare our results to investigations of cave percolation drip hydrology. Our observation of a drip recharge response within 7-days of rainfall is similar to that in caves with a depth less than 30 m below surface. Tooth and Fairchild (2003) observe a maximum 3-day lag in drip water recharge response at the ~20 m deep Crag Cave, Ireland; and at 27 m below ground surface at Mount Carmel, Israel, percolation waters were shown to respond within hours, with a peak hydrograph up to three days after rainfall (Arbel et al 2010). In contrast, at 61 m to 250 m below land surface, Williams (1983) reports drip hydrology responses up to 5 weeks after rainfall at Carlsbad Caverns, USA. Rainfall recharge thresholds for cave percolation waters have been less widely reported. Our rainfall recharge thresholds at South Glory Cave are lower than those determined for the arid Mount Carmel karst of Israel, where Lange et al (2010) report an irrigation experiment where 70 mm over 7- hours was not enough to generate recharge.

We can also compare our data to that of Genty and Deflandre (1998), who monitored one drip for five years from a Belgian cave system, and who showed a strong linear relationship ( $r = 0.97$ ) between total recharge and annual water excess (defined as P-PET) for a drip site with similar characteristics and total recharge amount to South Glory Cave. Conversely, from a similar analysis, we find Spearman's  $r_s$  correlations between 0.81 and  $-0.38$  (median  $r_s = 0.23$ ) for our drip sites, demonstrating that the heterogeneity of karst drip hydrology can lead to a more

complex relationship between water excess and recharge amount. This complexity also motivates a more in-depth analytical approach as the one introduced in this study.

Our approach can also be used to hindcast drip recharge amounts. This would assist researchers investigating the water oxygen isotope record, for example as a possible groundwater recharge indicator or as the drip water source for speleothem isotope archives. A hindcast recharge amount record could then be compared to drip water  $\delta^{18}\text{O}$  (at sites where this has been measured) to hindcast monthly and annual drip water  $\delta^{18}\text{O}$  over time. Or, using measured rainfall  $\delta^{18}\text{O}$  at a site (at sites where this has been measured), could be used to produce a hindcast of recharge-weighted  $\delta^{18}\text{O}$ .

Finally, at the Yarrangobilly Caves, our observation of no recharge occurring in March, suggests there will be an annual decoupling of stored and infiltrating waters. This could lead to an annual geochemical signature in recharge water e.g. Zn, K, Na, as observed in the adjacent Harrie Wood Cave (Tadros et al., 2019). Our cave drip water monitoring programme was carried out throughout a period of positive Southern Annular Mode, which generally brings wetter than average summers (Hendon et al., 2007). This suggests that the lack of March recharge is even more likely in a negative phase SAM. An annual flush of soil-derived elements in the first recharge events of the hydrological year (April) would be of use for geochemical applications if preserved in speleothems (Smith et al., 2009).

## 6. Conclusions

We have investigated the relationship between rainfall amount and cave percolation water time-series characteristics at the Glory Cave karst system (Yarrangobilly Caves, New South Wales) to determine rainfall recharge threshold amounts, and through simple water budget modelling, to determine soil and karst water storage volumes. The study is based on a novel multidisciplinary approach composed of the following steps. First, the percolation water entering the cave is measured at different points using multiple water drip loggers. Secondly, the obtained dataset is completed using a latest-generation statistical algorithm based on data-pattern reconstruction, to have a gap-free multivariate drip-rate time series. The final dataset shows different seasonal patterns and a detailed picture of the spatial heterogeneity of potential recharge inside the cave. The percolation water times series characteristics are used to determine rainfall recharge thresholds at various timescales using two different methodologies (total annual percolation water volume; hydrograph response). This estimation of rainfall recharge thresholds (daily and 7-day; annual average and monthly-average) has been corroborated by the estimation of the storage capacity of the karst system, quantified with a simple water budget model.

The proposed approach, relying on low-cost instrumentation and limited modelling efforts, has the potential of allowing a detailed observation of the spatiotemporal heterogeneity of potential recharge, observed as water percolating into cave environments. Future applications include a more accurate estimation of the recharge by means of remote sensing tools. Once the distribution of the relationship between annual recharge amount and precipitation above threshold value has been quantified for sufficient drip waters, upscaling using lidar mapping can quantify the total number of drip sources (Mahmud et al. 2016). This would allow a more reliable annual water balance estimation, based on the joint statistical analysis of rainfall and discharge time series, with the only requirement of a sufficiently long (multiple-year) observation period.

## CRedit authorship contribution statement

**Andy Baker:** Conceptualization, Data curation, Formal analysis, Funding acquisition, Investigation, Methodology, Project administration, Resources, Writing - original draft. **Mirjam Scheller:** Formal

analysis, Investigation, Methodology, Software, Visualization. **Fabio Oriani**: Conceptualization, Formal analysis, Investigation, Methodology, Software, Visualization, Writing - original draft. **Grégoire Mariéthoz**: Conceptualization, Funding acquisition, Methodology, Validation, Project administration. **Andreas Hartmann**: Conceptualization, Funding acquisition, Resources, Validation, Software, Supervision, Project administration. **Zhangyong Wang**: Data curation, Funding acquisition, Investigation. **Mark Cuthbert**: Conceptualization, Funding acquisition, Validation.

## Declaration of Competing Interest

The authors declare that they have no known competing financial interests or personal relationships that could have appeared to influence the work reported in this paper.

## Acknowledgements

AB acknowledges the support of the Herbet Foundation, University of Lausanne, and ZYW the support of the Chinese Scholarship Council (CSC). MS and AH were supported by the Emmy Noether-Programme of the German Research Foundation (DFG; grant number HA 8113/1-1; project 'Global Assessment of Water Stress in Karst Regions in a Changing World'). MOC gratefully acknowledges an Independent Research Fellowship from the UK Natural Environment Research Council (NE/P017819/1). We thank the management and staff at Yarrangobilly Caves for their continued support for karst research, Dr Katie Coleborn for drip logger data management until 2017, Tunde Olarinoye for managing the Github site, Andy Spate and Andrew Baker for their advice on the conceptual model, and Dr Pauline Treble (ANSTO) for encouraging research at Yarrangobilly. The review comments of Naomi Mazzilli and three anonymous reviewers are very much appreciated.

## Appendix A. Supplementary data

Supplementary data to this article can be found online at <https://doi.org/10.1016/j.jhydrol.2021.125965>.

## References

- Arbel, Y., Greenbaum, N., Lange, J., Inbar, M., 2010. Infiltration processes and flow rates in developed karst vadose zone using tracers in cave drips. *Earth Surface Proc. Landforms* 35, 1682–1693.
- Baker, A., Blyth, A.J., Jex, C.N., et al., 2019. Glycerol dialkyl glycerol tetraethers (GDGT) distributions from soil to cave: refining the speleothem paleothermometer. *Organ. Geochem.* 136, 103890.
- Baker, A., Berthelin, R., Cuthbert, M.O., et al., 2020. Rainfall recharge thresholds in a subtropical climate determined using a regional cave drip water monitoring network. *J. Hydrol.* 587, 125001.
- Barron, O.V., Crosbie, R.S., Dawes, W.R., et al., 2012. Climate controls on diffuse groundwater recharge across Australia. *Hydrol. Earth Syst. Sci.* 16, 4557–4570.
- Campbell, M., Callow, J.N., McGrath, G., McGowan, H., 2017. A multimethod approach to inform epikarst drip discharge modelling: implications for paleo-climate reconstruction. *Hydrol. Procs.* 31, 4734–4747.
- Coleborn, K., Rau, G.C., Cuthbert, M.O., et al., 2016. Solar forced diurnal regulation of cave drip rates via phreatophyte evapotranspiration. *Hydrol. Earth Syst. Sci.* 20, 4439–4455.
- Coleborn, K., Baker, A., Treble, P.C., et al., 2018. The impact of fire on the geochemistry of speleothem-forming drip water in a sub-alpine cave. *Sci. Total Environ.* 642, 408–420.
- Coleborn, K., Baker, A., Treble, P.C., et al., 2019. Corrigendum to "The impact of fire on the geochemistry of speleothem-forming drip water in a sub-alpine cave" [*Sci. Total Environ.* (2018) 408–420]. *Sci. Total Environ.* 668, 1339–1340.
- Collister, C., Matthey, D., 2008. Controls on water drop amount at speleothem drip sites: An experimental study. *J. Hydrol.* 358, 259–267.
- Crosbie, R.S., Jolly, I.D., Leaney, F.W., Petheram, C., 2010. Can the dataset of field based recharge estimates in Australia be used to predict recharge in data-poor areas? *Hydrol. Earth Syst. Sci.* 14, 2023–2038.
- Cuthbert, M.O., Baker, A., Jex, C.N., et al., 2014. Drip water isotopes in semi-arid karst: implications for speleothem paleoclimatology. *Earth Planet. Sci. Lett.* 395, 194–204.
- Dembélé, M., Oriani, F., Tumbulto, J., Mariéthoz, G., Schaeffli, B., 2019. Gap-filling of daily streamflow time series using Direct Sampling in various hydroclimatic settings. *J. Hydrol.* 569, 573–586.
- Frost, A.J. and Wright, D.P., 2018. Evaluation of the Australian Landscape Water Balance model: AWRA-L v6. Bureau of Meteorology Technical Report.
- Frost, A. J., Ramchurn, A. and Smith, A., 2018. The Australian Landscape Water Balance model (AWRA-L v6). Technical Description of the Australian Water Resources Assessment Landscape model version 6. Bureau of Meteorology Technical Report.
- Genty, D., Deflandre, G., 1998. Drip flow variations under a stalactite of the Pere Noel cave (Belgium). Evidence of seasonal variations and air pressure constraints. *J. Hydrol.* 211, 208–232.
- Gravey, M., Mariéthoz, G., 2020. QuickSampling v1.0: a robust and simplified pixel-based multiple-point simulation approach. *Geosci. Model Dev.* 13, 2611–2630.
- Hartmann, A., Barberá, J.A., Lange, J., et al., 2013. Progress in the hydrologic simulation of time variant recharge areas of karst systems – Exemplified at a karst spring in Southern Spain. *Adv. Water Resour.* 54, 149–160.
- Healy, R.W., 2010. Estimating groundwater recharge. Cambridge University Press.
- Heilman, J.L., Litvak, M.E., McInnes, K.J., et al., 2014. Water-storage capacity controls energy partitioning and water use in karst ecosystems on the Edwards Plateau, Texas. *Ecohydrology* 7, 127–138.
- Hendon, H.H., Thompson, D.W.J., Wheeler, M.C., 2007. Australian rainfall and surface temperature variations associated with the Southern Hemisphere Annular Mode. *J. Clim.* 20, 2452–2467.
- Jasechko, S., 2019. Global isotope hydrogeology – review. *Rev. Geophys.* 57, 835–965.
- Lange, J., Arbel, Y., Grodek, T., Greenbaum, N., 2010. Water percolation process studies in a Mediterranean karst area. *Hydrol. Process.* 24, 1866–1879.
- Mahmud, K., Mariéthoz, G., Treble, P.C., Baker, A., 2016. Terrestrial LiDAR survey and morphological analysis to identify infiltration properties in the Tamala Limestone, Western Australia. *IEEE JSTARS* 8, 4871–4881.
- Markowska, M., Andersen, M.S., Treble, P.C., et al., 2015. Unsaturated zone hydrology and cave drip discharge water response: implications for speleothem palaeoclimate record variability. *J. Hydrol.* 529, 662–675.
- McGowan, H., Callow, J.N., Soderholm, J., et al., 2018. Global warming in the context of 2000 years of Australian alpine temperature and snow cover. *Sci. Rep.* 8, 4398.
- Olarinoye, T., Gleeson, T., Marx, V., et al., 2020. Global karst springs hydrograph dataset for research and management of the world's fastest-flowing groundwater. *Sci. Data* 7. <https://doi.org/10.1038/s41597-019-0346-5>.
- Oriani, F., Borghi, A., Straubhaar, J., et al., 2016. Missing data simulation inside flow rate time-series using multiple-point statistics. *Environ. Model. Software* 86, 264–276.
- Oriani, F., Straubhaar, J., Renard, P., Mariéthoz, G., 2014. Simulation of rainfall time-series from different climatic regions using the Direct Sampling technique. *Hydrol. Earth Syst. Sci.* 11, 3213–3247.
- Peel, M.C., Finlayson, B.L., McMahon, T.A., 2007. Updated world map of the Köppen-Geiger climate classification. *Hydrol. Earth Syst. Sci.* 11, 1633–1644.
- Scanlon, B., Healy, R., Cook, P., 2002. Choosing appropriate techniques for quantifying groundwater recharge. *Hydrogeol. J.* 10, 18–39.
- Schmidt, S., Geyer, T., Guttman, J., et al., 2014. Characterisation and modelling of conduit restricted karst aquifers – example of the Auja spring, Jordan Valley. *J. Hydrol.* 511, 750–763.
- Smith, C.L., Fairchild, I.J., Spötl, C., et al., 2009. Chronology-building using objective identification of annual signals in trace element profiles of stalagmites. *Quatern. Geochron.* 4, 11–21.
- Spate, A.P., Jennings, J.N., Smith, D.I., Greenaway, M.A., 1977. A triple dye tracing experiment at Yarrangobilly. *Helveticite* 14, 27–48.
- Tadros, C.V., Treble, P.C., Baker, A., et al., 2016. ENSO - cave drip water hydrochemical relationship: a 7-year dataset from south-eastern Australia. *Hydrol. Earth Syst. Sci.* 20, 4625–4640.
- Tadros, C.V., Treble, P.C., Baker, A., et al., 2019. Cave drip water solutes in south-eastern Australia: constraining sources, sinks and processes. *Sci. Total Environ.* 651, 2175–2186.
- Tooth, A.F. & Fairchild, I.J. 2003 Soil and karst aquifer hydrological controls on the geochemical evolution of speleothem-forming drip waters, Crag Cave, southwest Ireland. *J. Hydrol.*, 273, 51–68.
- Viney, N., Vaze, J., Crosbie, R., et al., 2015. AWRA-L v5.0: technical description of model algorithms and inputs. CSIRO, Australia.
- Williams, P.W., 1983. The role of the subcutaneous zone in karst hydrology. *J. Hydrol.* 61, 45–67.